# Exploring Transporters within the Small Multidrug Resistance Family Using Solid-State NMR Spectroscopy

Nathaniel J. Traaseth, James R. Banigan & Maureen Leninger

*New York University, New York, NY, USA*

Small multidrug resistance (SMR) proteins comprise a family of bacterial secondary active transporters that confer drug resistance to antiseptics and antibiotics. EmrE has emerged as the model protein of the SMR family and an archetype to understand the ion-coupled transport mechanism. The importance of EmrE is further underscored by its proposed role as an evolutionary predecessor to larger transporters, which stems from the similarity of the antiparallel and asymmetric structure of the EmrE dimer with the *inverted repeat* fold of efflux pumps within other transport families such as the major facilitator superfamily. This review describes progress to reveal the atomic-scale structure and dynamics of SMR proteins determined under native-like conditions in lipid bilayers using solid-state NMR spectroscopy. The combination of MAS and oriented solid-state NMR approaches developed to study the SMR family serves as a framework for future efforts to uncover structural details of other secondary active transporters that are abundant in biology.

**Keywords:** small multidrug resistance family, EmrE, membrane proteins, protein conformational dynamics, solid-state NMR spectroscopy

**How to cite this article:**
*eMagRes*, 2015, Vol 4: 551–560. DOI 10.1002/9780470034590.emrstm1413

## Introduction

The small multidrug resistance (SMR) family is comprised of membrane protein transporters with four transmembrane (TM) domains and 100 to 140 residues in length. These efflux pumps are able to transport a wide range of quaternary cation compounds, dyes, and other antiseptics across the cell membrane using the proton motive force.[1,2] EmrE is the most studied protein in the SMR family with a significant number of biochemical and structural experiments carried out. One of the most interesting features of EmrE is its adoption of a dual topology, in that it is inserted into the membrane with two distinct orientations.[3–5] This feature allows for the formation of the antiparallel dimer structure in biological membranes, which was determined using cryo-electron microscopy and X-ray crystallography,[6–8] and links the protein's insertion pathway to the fold of the native structure. It is important to note that the structural models have been validated with a number of different techniques including chemical crosslinking, NMR spectroscopy, EPR spectroscopy, and single-molecule fluorescence resonance energy transfer (FRET) experiments.[9–14]

This review focuses on the progress made from a solid-state nuclear magnetic resonance (SSNMR) perspective to describe structure and dynamics of EmrE in a native-like lipid bilayer environment in the drug-free and drug-bound forms. Indeed, the ideal system for studying membrane proteins is a lipid bilayer that closely mimics the physical properties of the cellular membrane environment.[15] For these reasons, the use of SSNMR spectroscopy has emerged as a preferred method for studying membrane proteins. Within the SSNMR field, there are two major subdivisions: (i) uniaxial alignment of the proteins relative to the magnetic field and (ii) unoriented liposome or nanodisc preparations. The former describes oriented solid-state nuclear magnetic resonance (O-SSNMR) where the anisotropic chemical shifts and dipolar couplings are recorded to determine the backbone structure and tilt angles of the protein's secondary structures relative to the lipid bilayer.[16–28] Alternative methods have been developed to probe tilt angle geometries of the protein in unaligned lipid bilayers.[29–31] The criterion for this method is fast uniaxial rotational diffusion with respect to the lipid bilayer normal. While these methods can be used to study smaller membrane proteins, recent findings suggest that this approach may not have broad applicability to larger polytopic membrane proteins that undergo intermediate timescale motion above the main phase transition of the lipid bilayer.[32,33]

Membrane proteins in unaligned proteoliposomes can also be studied at atomic resolution through the use of MAS spectroscopy.[34–39] The principle behind MAS is to mechanically rotate the sample at the magic-angle, which removes a portion of the anisotropy and in the process reduces the spectral complexity resulting in narrow resonances.[40,41] The MAS and oriented methods provide complementary structural information and have been used in a synergistic manner to obtain hybrid backbone and side-chain structures of membrane proteins.[18,19,31,42] In addition, both MAS and O-SSNMR are capable of capturing the wide range of dynamics that membrane proteins experience within the bilayer, including

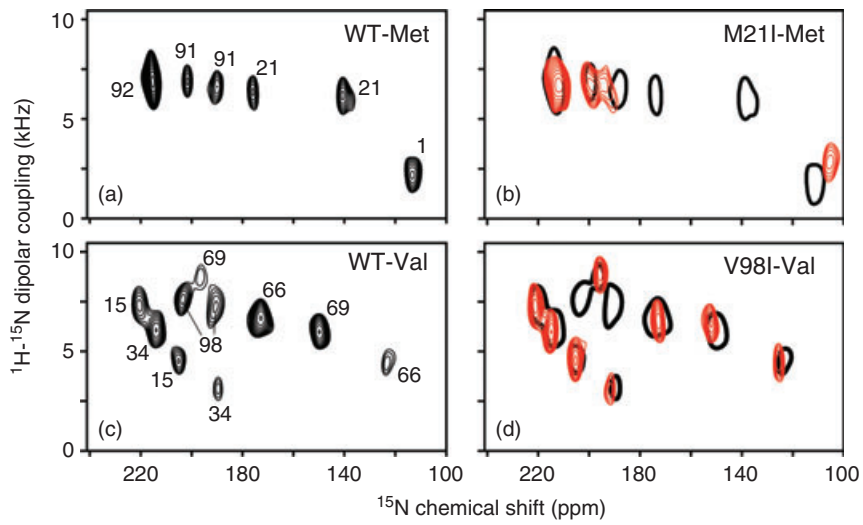


**Figure 1.** (a, c) Sensitivity-enhanced PISEMA[49] spectra of [$^{15}$N-Met] and [$^{15}$N-Val] selectively labeled EmrE. (b, d) Assignments were obtained with single-site mutant samples (red). The spectra in panels (b) and (d) also show the wild-type dataset (black outline). (Reproduced with permission from Ref. 10. © WILEY-VCH Verlag GmbH & Co. KGaA, Weinheim, 2013)

uniaxial rotational motion, wobbling, and other conformational dynamics at the backbone and side chains.[28,35,38,43–48] The following sections highlight the discoveries made in the SMR family using SSNMR spectroscopy in lipid bilayers and bicelles.

## Asymmetric Structure of Drug-Free EmrE Relative to the Lipid Bilayer

Molecular transporters require conformational fluctuations within the bilayer to accommodate the movement of substrates across the membrane. For this reason, O-SSNMR experiments such as PISEMA can be a valuable approach for directly mapping the associated angular changes in the substrate-free and bound forms of the protein. Our laboratory has acquired several PISEMA experiments using isotopically enriched EmrE reconstituted into magnetically aligned lipid bicelles consisting of DMPC/DHPC (3.2/1, mol/mol). The bilayer normal was oriented in a parallel direction with respect to the magnetic field through the addition of $YbCl_3$. To resolve site-specific changes within the structure, EmrE was selectively labeled with [$^{15}$N-Val] and [$^{15}$N-Met] with the corresponding PISEMA spectra for the drug-free protein shown in Figure 1. These spectra indicate peak doubling relative to the number of residues in the primary sequence (e.g., 5 valine residues and 10 peaks) and clearly show at atomic-resolution that the two monomers in the dimer have asymmetric tilt and rotation angles with respect to the lipid bilayer consistent with low-resolution images from cryo-electron microscopy.[6,7] To obtain the assignments, we engineered single-site Val to Ile mutants or Met to Leu mutants and carried out the same selective labeling. The spectra corresponding to the single-site mutants gave two fewer peaks relative to the wild-type data and validated the peak-doubling observation and provided an unambiguous way to obtain the assignments. Note that Met-1 and Met-92 gave only a single peak in the PISEMA spectrum, which is explained by the position at the N-terminus (i.e., dynamic averaging) and similarity of the two monomer geometries in TM4, respectively.

The valine and methionine assignments provided useful site-specific probes of atomic-scale changes occurring within each helix of EmrE. For example, the upfield chemical shifts for Val-66 and Val-69 within monomer B of TM3 supported the conclusion that this helix was the most tilted in the bilayer. Insight into TM1 helices that contain the essential Glu-14 residue for proton and drug transport in EmrE[50] was provided by measurements for Val-15 and later spectra of Thr-18 and Thr-19 which enabled us to obtain best-fit helical tilt angles of 16° and 33° for the two TM1 helices.[9] The different tilt angles support the asymmetric dimer structure of EmrE. The least tilted helices within EmrE were found to be those of TM4. This is seen by the resonances for Met-91, Met-92, and Val-98, which have $^{15}$N chemical shift frequencies of 190–215 ppm and $^{1}$H–$^{15}$N dipolar couplings of 6–8 kHz. While the PISEMA-derived tilt angles are in agreement with the backbone model of EmrE (~12–14° for each[51]), the rotation angles differed by ~33° and 50° for the two monomers.[10]

## Drug Binding to a Conserved Glutamate Residue Observed with MAS

The most important and conserved residue in the SMR family is an anionic glutamate found in TM1 that is responsible for proton and drug transport.[50] Glaubitz and coworkers obtained direct insight into this key residue of *Escherichia coli* EmrE (Glu-14) through preparation of a selectively labeled glutamate sample using the cell-free approach to avoid isotopic scrambling.[14] The only other glutamate residue in the primary

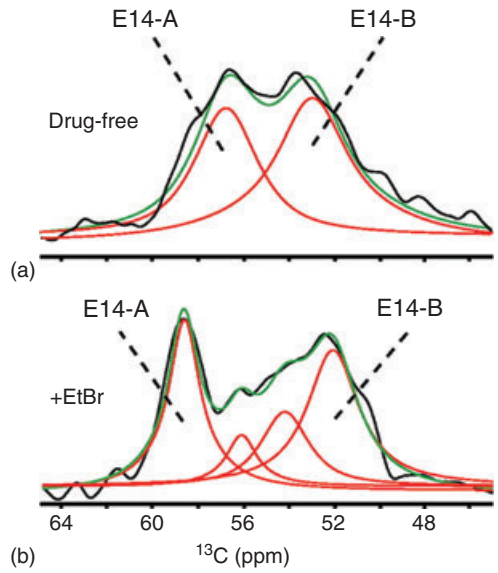


**Figure 2.** $^{13}$C MAS-NMR spectra of EmrE reconstituted into *E. coli* lipids. Residue E14 was selectively $^{13}$C-labeled. In the apo-state, the C$\alpha$ resonance splits into two equal populations (a), which both shift upon saturation with ethidium (b). (Reproduced from Ref. 52. With kind permission from Springer Science and Business Media)

sequence was mutated to Ala (E25A), which enabled unambiguous assignment for Glu-14 from 1-D $^{13}$C CP-MAS and 2-D $^{13}$C/$^{13}$C double-quantum/single-quantum correlation experiments in the drug-free and ethidium-bound forms. The spectra were obtained at a temperature of 200 K and gave two peaks in the drug-free state (Figure 2a), which was attributed to the structural inequivalency of the substrate chamber. These findings are in agreement with the structural asymmetry observed in the cryoelectron microscopy images[6,7] and O-SSNMR experiments in the absence of drug.[10] Upon addition of ethidium, the two most intense peaks in the spectrum became narrower and suggested a decreased amount of structural heterogeneity in the drug-bound form of the protein (Figure 2b). It is possible that the spectral broadening in the drug-free form of EmrE stemmed from trapping several conformational states that have been reported for the drug-free form of the protein.[9]

To obtain direct evidence that Glu-14 was responsible for drug binding in EmrE, Ong *et al.*[13] used DNP in combination with MAS to probe contacts between Glu-14 of EmrE and the tetraphenylphosphonium ($TPP^+$) substrate. In the DNP approach, the sensitivity is greatly enhanced by the transfer of polarization from electrons. In these experiments, EmrE was selectively labeled using [2-$^{13}$C] glycerol and $TPP^+$ was synthesized with a single phenyl ring labeled with $^{13}$C. Two-dimensional $^{13}$C/$^{13}$C dipolar assisted rotational resonance (DARR) correlation spectra revealed cross-peaks between EmrE and $TPP^+$ with the DNP enhancing the signal/noise by 19-fold at a temperature of 100 K (Figure 3). The observed cross-peaks were assigned to arise from contacts between the $C_\delta$ of Glu-14 and the *meta*, *para*, and *ortho* carbons in $TPP^+$ and were consistent with an earlier study using $^{31}$P CP-MAS which suggested a specific interaction between EmrE and $TPP^+$.[53]

The strongest correlation observed was between $C_\delta$ and the *meta* position and was estimated to have a distance of ~6 Å,[13] which is in agreement with the proposed EmrE assembly from the $TPP^+$-bound crystal structure[8] and mutational studies emphasizing the importance of Glu-14 for binding.[50] While the spectral resolution at 100 K did not enable the authors to distinguish multiple peaks for the two Glu-14 residues in the binding pocket, future experiments will likely provide additional insight into the binding pocket by resolving distances to each monomer within the asymmetric dimer.

## Drug Binding Leads to Conformational Changes with Respect to the Bilayer

Drug binding has been found to induce conformational changes as probed through electron microscopy.[54,55] To investigate these structural changes at higher resolution, our laboratory recorded PISEMA spectra of EmrE in the presence of $TPP^+$ in magnetically aligned bicelles.[10] These experiments were performed in a similar manner as those for the drug-free state described earlier. Upon addition of $TPP^+$, we observed no major chemical shift changes for TM4, which is in agreement with the hypothesis that this helix imparts dimer stability and does not undergo tilt angle changes upon drug binding. This is consistent with mutational studies on EmrE and other SMR homologues[12,56,57] and is consistent with recent results from our laboratory that show no chemical shift perturbations to the loop adjoining TM3 with TM4 upon addition of $TPP^+$.[58] Similar to TM4, we did not observe significant perturbations for Val-15 and Met-21 upon drug binding ($\leq$3 ppm in $^{15}$N), which suggested that TM1 did not have tilt angle changes with respect to the lipid bilayer. One possible interpretation is that TM1 is anchored in order to position Glu-14 side chains in an appropriate orientation for drug and proton binding. In contrast, large structural changes were found for residues Val-66 and Val-69 within TM3. Interestingly, $TPP^+$ had a differential effect on each monomer: Val-66 on one monomer showed a large perturbation with no change to Val-69, while the other monomer displayed a change to Val-69 and no peak movement for Val-66 (Figure 4a–c). These perturbations can be approximated as a differential bend within TM3 that would likely occur at a conserved Gly-X-Gly motif present at positions 65–67 in the primary sequence (Figure 4d). We propose that the malleability of this essential motif is critical for imparting structural plasticity to binding a wide range of distinct drugs.[10]

To quantitatively compare our experimental observables with the available structural data, we calculated PISEMA spectra from the backbone structural model of EmrE derived from cryo-electron microscopy and cross-linking restraints (*pdb 2I68*).[51] This model was constructed using ideal helices for seven out of eight TM domains in the dimer. Interestingly, the only deviation from ideality was for TM3 near the Gly-X-Gly motif,[51] which is consistent with the bending location identified in the PISEMA experiments. The comparison of experimental and calculated values is shown in Figure 4(e). Overall the agreement between the two is quite good and further supports the asymmetric and antiparallel dimer structure of EmrE.

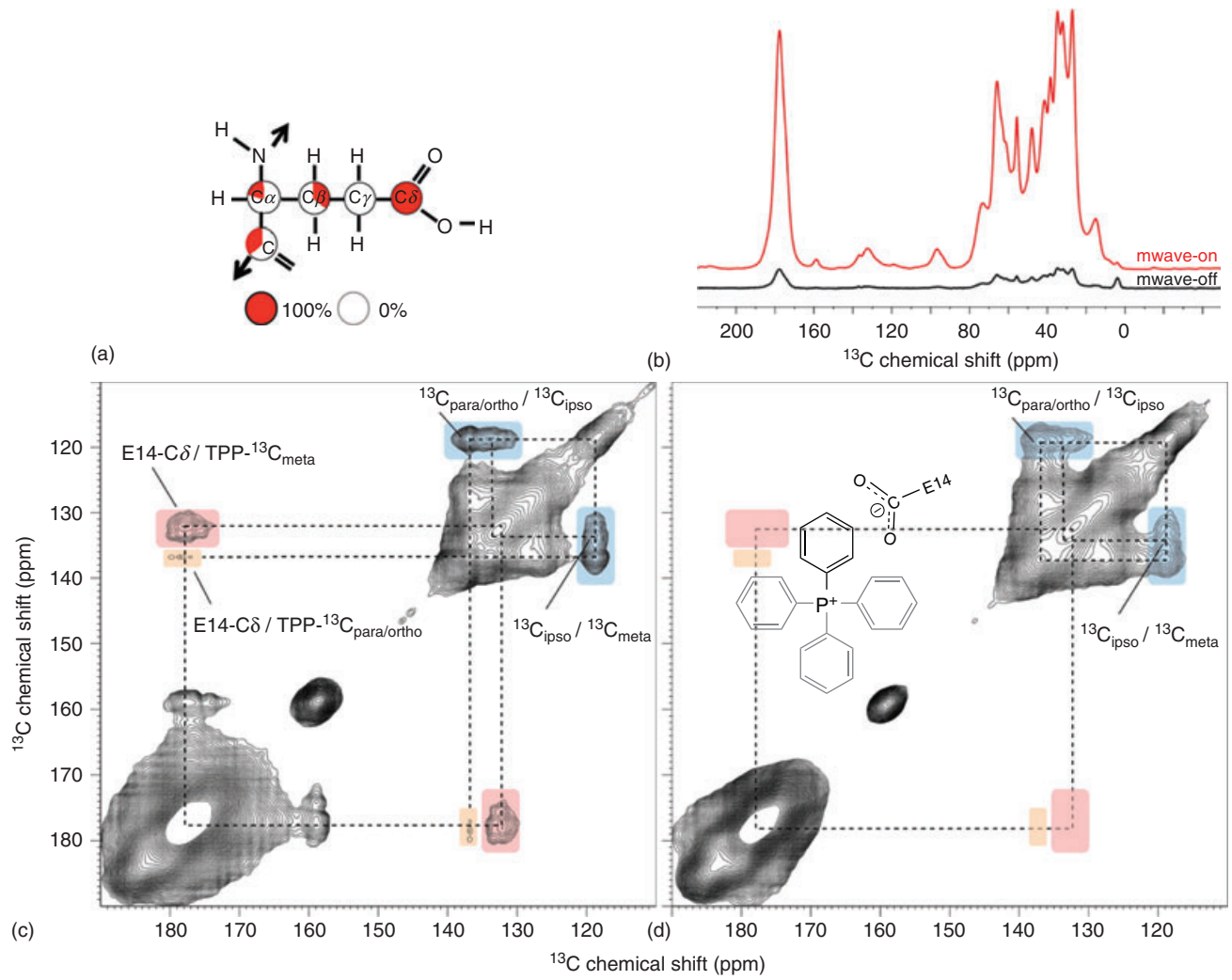


**Figure 3.** The $TPP^+$-EmrE contacts probed by dynamic nuclear polarization MAS-SSNMR. (a) $^{13}$C-labeling pattern of glutamate residues within EmrE from using 2-$^{13}$C-glycerol as the sole carbon source. The red circle indicates the completeness of $^{13}$C incorporation at the given carbon. (b) 20 mM TOTAPOL with DNP resulted in 19-fold signal/noise enhancement at a temperature of 100 K. (c) A $^{13}$C/$^{13}$C 300 ms DARR experiment showed specific correlations between Glu-14 and the $^{13}$C-labeled $TPP^+$. (d) The same DARR experiments as in (c) with EmrE not enriched with $^{13}$C at Glu-14. (Reprinted with permission from Ong, Y. S.; Lakatos, A.; Becker-Baldus, J.; Pos, K. M.; Glaubitz, C. Detecting substrates bound to the secondary multidrug efflux pump EmrE by DNP-enhanced solid-state NMR. J Am Chem Soc 2013, 135, 15754–15762. Copyright (2013) American Chemical Society)

## Conformational Dynamics of EmrE in Aligned Lipid Bicelles

The most prevalent model to explain secondary active transport is the alternating access model,[59] which involves exchange between two conformations open to opposite sides of the membrane (see schematic in Figure 5a). In the antiport mechanism, the binding of either protons or drugs induces a structural change resulting in the movement of substrates across the membrane.[61,62] The favorable proton transport drives the movement of drugs from the cytoplasm to the periplasm in the SMR family.[2,63] It has recently been shown that blocking the conformational movement between inward-open and outward-open states results in the failure of EmrE to transport substrates.[64] Henzler-Wildman and coworkers observed that the rate from inward-open to outward-open states for $TPP^+$-bound EmrE was $\sim 5\,s^{-1}$ at 45 °C using solution NMR spectroscopy[11] and followed up on this initial study by determining exchange rates for several other drugs.[65] To obtain insight into the dynamics of the drug-free form, we carried out exchange experiments in aligned lipid bicelles.[9] An advantage of our O-SSNMR approach was the large chemical shift difference between the two populations owing to the anisotropic nature of chemical shifts and dipolar couplings in the aligned sample. In fact, at 37 °C the solution NMR spectrum for drug-free EmrE at pH 6.9 was broadened as a result of chemical exchange on the intermediate timescale. However, in PISEMA spectroscopy the two populations were resolved and separated by as much as 40 ppm in the $^{15}$N dimension.[9] As the

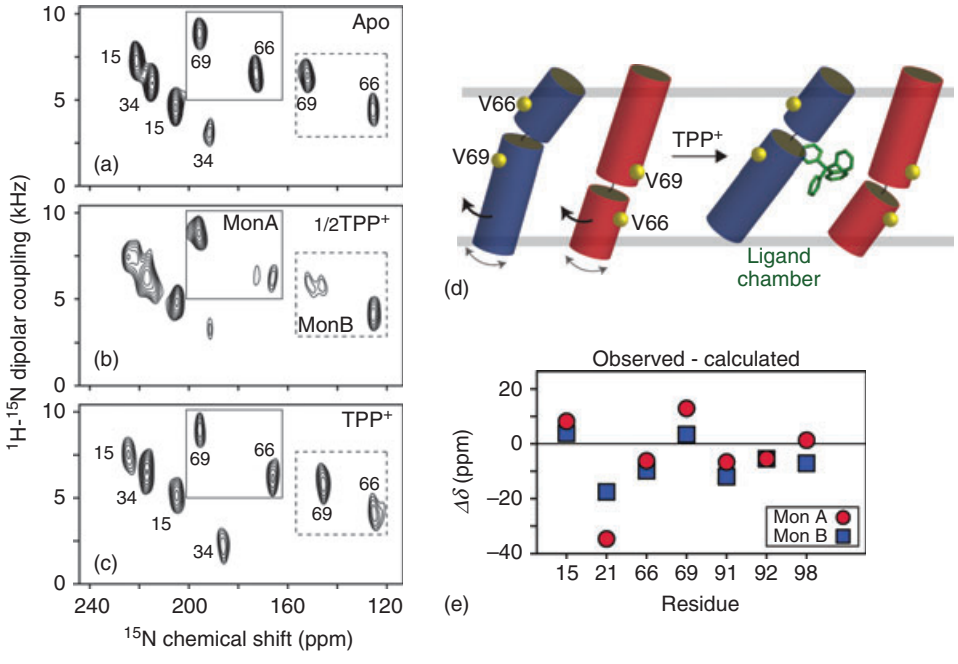


**Figure 4.** Drug-induced conformational change of EmrE probed with O-SSNMR. PISEMA spectra are shown for [$^{15}$N-Val] V98I with the following ratios of $TPP^+$ relative to the EmrE dimer: (a) 0:1, (b) 0.5:1, and (c) saturating drug. (d) Model of TM3 bending motion consistent with the differential behavior of Val-66 and Val-69 in monomers A and B in the PISEMA spectra shown in panels (a) through (c). (e) Calculated chemical shifts from the computational model of EmrE by Fleishman *et al.*[51] vs observed anisotropic chemical shifts for Met and Val residues. Note that Val34 does not have a calculated chemical shift owing to a missing residue preceding it in the structural model. (Reproduced with permission from Ref. 10. © WILEY-VCH Verlag GmbH & Co. KGaA, Weinheim, 2013)

isotropic chemical shift differences were typically ~1 ppm in the solution NMR experiments, the larger frequency splitting shifted the exchange regime to the slow timescale and enabled us to accurately quantify the exchange process with the use of $T_{1zz}$ experiments. As seen in Figure 5(b), we used a 2-D $^{15}$N/$^{15}$N proton-driven spin diffusion (PDSD) experiment for selectively [$^{15}$N-Thr] labeled EmrE and observed significantly stronger cross-peaks for EmrE in the absence of drug compared to the $TPP^+$ bound form. The quantification of the exchange rates were carried out using a novel application of the PUREX[60] approach that employed a variable mixing period in combination with difference spectroscopy, which enabled the dynamics to be monitored from 1-D spectra. Curve-fitting the data allowed us to determine that drug-free EmrE converted from an inward-open to outward-open state ~50-fold faster than the $TPP^+$-bound state (Figure 5c; 175 $s^{-1}$ vs 3.2 $s^{-1}$).[9] The conformational flexibility displayed by EmrE suggests that the broad specificity toward drugs is encoded by the malleability of the structure. It is important to note that our experiments were carried out at slightly acidic pH value and thus Glu-14 was predominantly in the protonated form. Future efforts will seek to quantify the conformational exchange differences between EmrE in the Glu-14 protonated and deprotonated forms in order to provide additional insight into the transport cycle.

## Toward a Complete Structural Characterization of SMR Proteins Using MAS: Methods to Improve Spectral Resolution in Lipid Bilayers

A complete structural characterization of EmrE in lipid bilayers will require the usage of MAS experiments to probe distances and dihedral angles at all sites of the protein. The first MAS experiments aimed at EmrE were carried out by Reif and coworkers who obtained spectra for [U-$^{13}$C,$^{15}$N] EmrE in DMPC liposomes.[66] While several datasets were collected with EmrE and a single-site mutant (E14C) to assign Glu-14, the main challenge noted by the authors was the lack of spectral resolution,[66] which is a known problem for helical membrane proteins that have similar chemical shifts and significant spectral overlap. For this reason, novel methods are necessary to resolve distinct peaks and obtain site-specific structural and dynamic information. With the hopes of finding a solution to this problem, our laboratory has developed new filtering tools to reduce the spectral congestion of inherently overlapped spectra. One of the methods we proposed and refer to as *afterglow spectroscopy* uses residual magnetization from the $^{15}$N–$^{13}$C cross-polarization[67,68] to generate a second multidimensional dataset in a sequential fashion.[69] Note that the term afterglow was inspired by the naming convention developed for solution NMR experiments.[70] In addition to the sensitivity gains, the afterglow method can be used as a filtering approach by

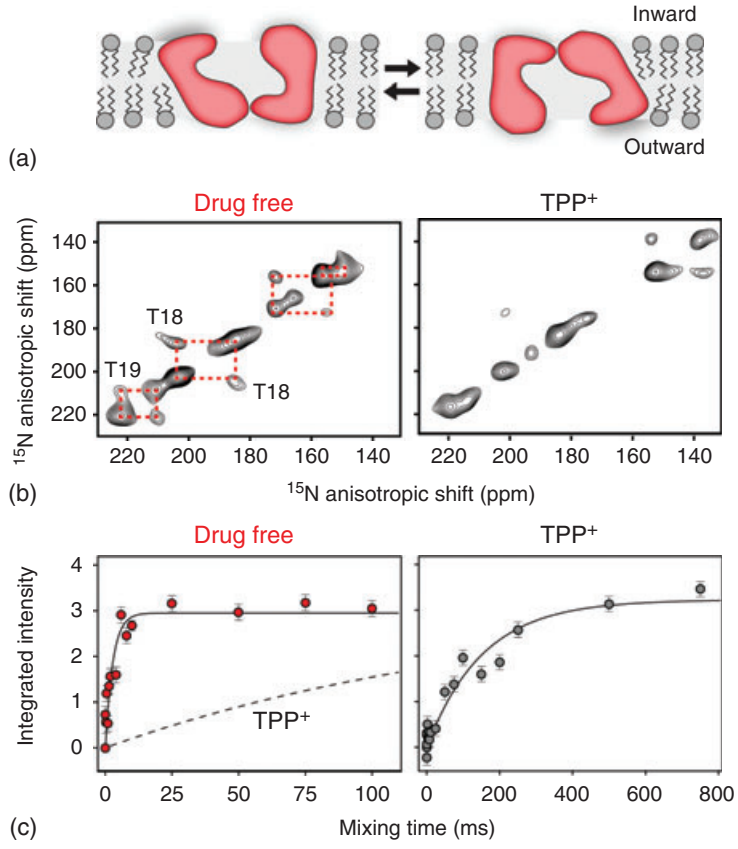


**Figure 5.** Conformational exchange probed by O-SSNMR in magnetically aligned bicelles. (a) Model depiction of inward-open to outward-open conformational exchange. (b) 2-D $^{15}N/^{15}N$ PDSD of [$^{15}N$-Thr] in the drug-free and $TPP^+$ bound forms. The cross-peaks in the drug-free spectrum were more intense relative to the $TPP^+$ bound state and indicative of faster conformational exchange. (c) The PUREX method[60] was used to quantify exchange rates by recording 1-D spectra for various mixing times, leading to ~50-fold faster exchange in drug-free EmrE than the $TPP^+$ bound form. (Reprinted with permission from Cho, M. K.; Gayen, A.; Banigan, J. R.; Leninger, M.; Traaseth, N. J. Intrinsic conformational plasticity of native EmrE provides a pathway for multidrug resistance. J Am Chem Soc 2014, 136, 8072–8080. Copyright (2014) American Chemical Society)

incorporating a $^{15}N$-labeled residue in otherwise uniformly $^{13}C$, $^{15}N$-labeled protein to identify residues that precede the $^{15}N$ amino acid (schematic shown in Figure 6a).[71] For example, we acquired an NCOCX afterglow experiment using a [$^{15}N$-Leu, U-$^{13}C$,$^{15}N$, natural-abundance Ile] sample of EmrE (revIL) to identify all residues preceding Leu in the primary sequence (Figure 6b). The reduction in spectral complexity simplified the resonance assignment process. In addition, we have employed a second filtering method, frequency-selective dipolar recoupling (FDR)-NCA spectroscopy[72]) to highlight residues appearing after reverse labeled amino acids (Figure 6e).[71] With the revIL sample, the FDR-NCA was used to probe only the residues appearing after Ile and Leu in the primary sequence. Similar to the afterglow method, the FDR-NCA also reduced the spectral congestion and allowed for site-specific assignments of EmrE.[71] The primary benefits of these two filtering methods are the simplicity in preparing reverse-labeled samples and the excellent sensitivity of the experiments compared to the standard heteronuclear datasets (e.g., NCA or NCO).

Another way we have improved the feasibility to characterize the structure of SMR proteins has been to enhance the spectral resolution through a careful optimization of temperature.[32] It is known that the most efficient cross-polarization transfers and often the best overall sensitivity are achieved when samples are rigid and frozen. The same is true for our studies of EmrE as seen in CP-MAS 1-D spectra as a function of temperature (Figure 7a,c). The plots of signal/noise vs temperature gave a sigmoidal shape where sensitivity decreased as the temperature was increased. However, sensitivity is not the only consideration; one needs to equally consider spectral resolution when setting up the experiment. In fact, we have found dramatic improvements in the spectral quality for somewhat small changes in the sample temperature (Figure 7b). For two SMR proteins (EmrE and SugE) in dimyristoylphosphatidylcholine (DMPC) lipid bilayers, we noticed that the peaks in the NCA 2-D correlation spectra were progressively broader at temperatures below 0 °C (Figure 7b), which is similar to the inhomogeneous line broadening noted for other proteins. The optimal spectral resolution was obtained at ~9 °C, which is intermediate with respect to the freezing temperature of water and the main phase transition of DMPC (23 °C). Temperatures above 9 °C led to significant broadening owing to whole-body uniaxial rotational diffusion around the bilayer normal that interfered with MAS. These results emphasize the importance of finding a temperature that gives optimal resolution while

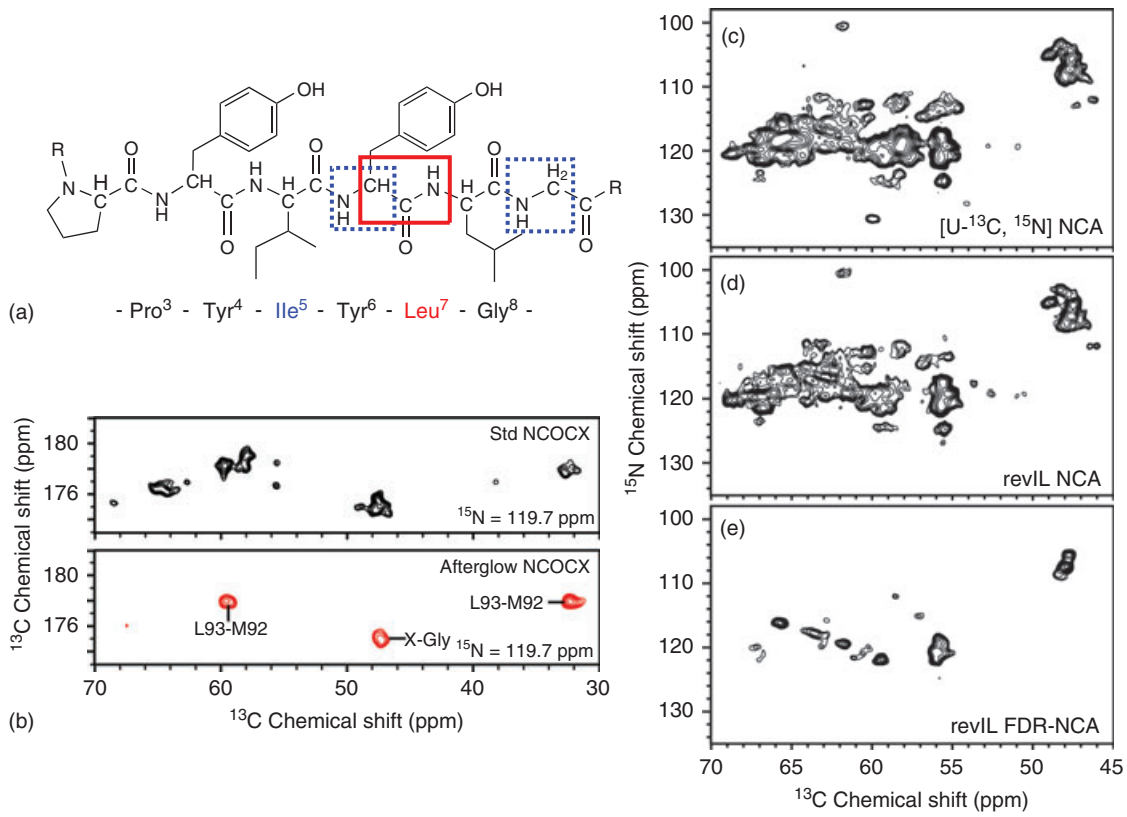


**Figure 6.** Afterglow techniques improve the resolution of MAS-SSNMR spectra for SMR proteins. (a) Schematic representation of afterglow methodologies.[69,71,72] Afterglow-NCOCX experiments with $^{15}$N reverse labeling highlights *i-1* residues with respect to the $^{15}$N labeled amino acid (e.g., X-$^{15}$Leu residues for the revIL sample; thick solid red box). The FDR-NCA can be used to highlight residues *i+1* relative to the reverse labeled sites (e.g., Ile-X and Leu-X pairs for the revIL sample; dotted blue boxes). (b) Comparison of a standard NCOCX for [U-$^{13}$C,$^{15}$N] EmrE and an afterglow NCOCX for revIL EmrE. The afterglow-NCOCX allows for facile identification of X-Leu spin systems. (c) NCA obtained with SPECIFIC-CP[67] of [U-$^{13}$C,$^{15}$N] EmrE. (d) NCA of revIL EmrE. (e) The FDR-NCA of revIL showing the reduction of spectral congestion relative to panel (d). (Reproduced from Ref. 71. With kind permission from Springer Science and Business Media)

providing for acceptable sensitivity to enable multidimensional acquisitions of high-quality data.[32]

## Future Directions

The success of crystallography over the last decade in resolving structures of secondary active transport proteins has been remarkable. However, a complete understanding of how these proteins function will require structural and biochemical validation in lipid bilayers. EmrE is a good example of this sentiment, with a wide variety of techniques converging in support of an anti-parallel and asymmetric structure of the protein within lipid membranes. We anticipate that the NMR tools used to study EmrE will provide a roadmap for mechanistic studies of larger transporters in biology. Future directions should aim at elucidating new structural models in lipid bilayers and resolving site-specific dynamics of these essential biomolecules that will provide for a more detailed understanding of transport mechanisms at the atomic level. We envision that this task will best be accomplished with a combination of solution and SSNMR (MAS and O-SSNMR) technologies. While the ability to characterize proteins in lipid bilayers using SSNMR is most desirable, solution NMR studies carried out in membrane mimics that do not interfere with structure (e.g., bicelles or nanodiscs) will continue to play a key role in unveiling the dynamic portrait of membrane proteins. Coupled with new NMR developments and careful optimization of sample preparation, the mechanistic details of transport will emerge in the near future.

## Acknowledgments

This work was supported by NIH grant R01AI108889. J.R.B. acknowledges support from a Dean's Dissertation Fellowship and M.L. is supported by a Margaret-Strauss Kramer Fellowship.

## Biographical Sketches

Nathaniel Traaseth is an Assistant Professor in the Department of Chemistry at New York University. He received his undergraduate degrees (BS in Chemistry, BS in Biochemistry and Molecular Biology,

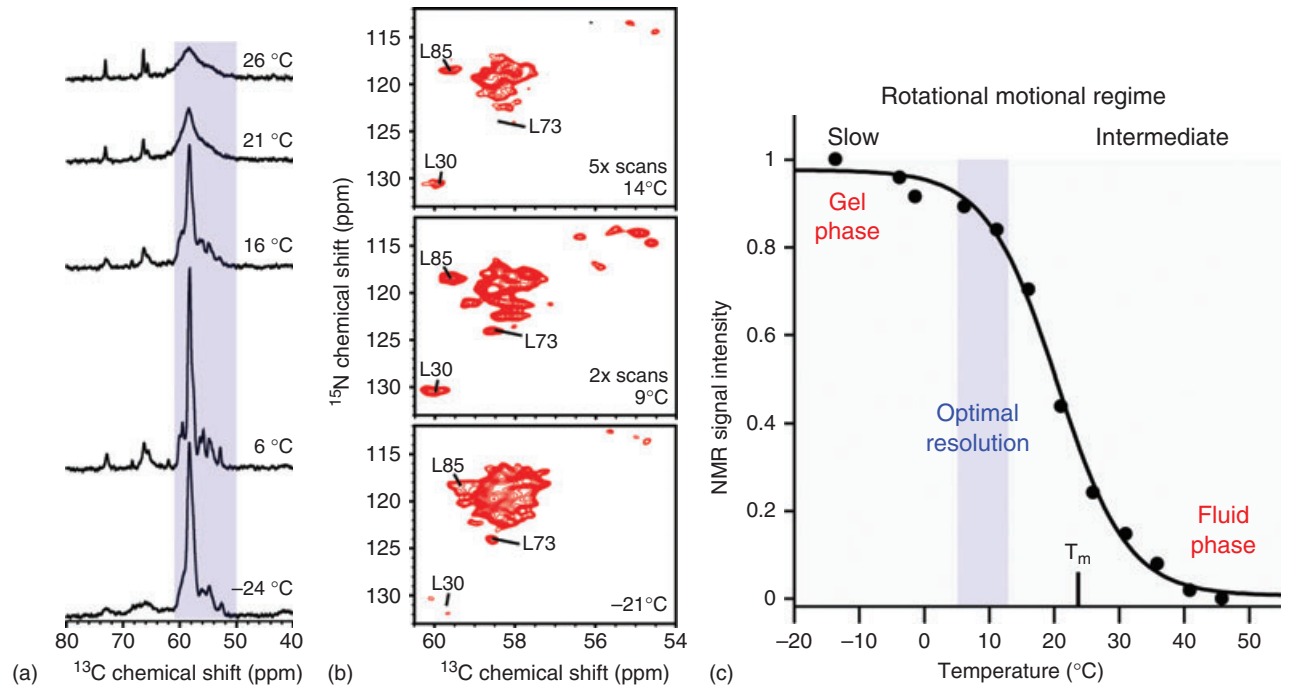


**Figure 7.** Effect of temperature on MAS-SSNMR sensitivity and spectral resolution for SMR proteins. (a) 1-D $^{1}H-^{13}C$ cross-polarization experiment as a function of temperature with [2-$^{13}C$,$^{15}N$-Leu] labeled EmrE. (b) 2-D NCA spectra of [2-$^{13}C$,$^{15}N$-Leu] EmrE at the given temperatures. At temperatures below the freezing point of water, inhomogeneous line broadening reduced the resolution. The optimal resolution was achieved at a temperature higher than the value of maximum sensitivity, but lower than the lipid melting temperature that led to significant reduction in signal intensity owing to uniaxial rotational diffusion relative to the lipid bilayer. (c) Integrated signal intensities from 1-D spectra derived from data in (a). (Reprinted from Biochim Biophys Acta, Banigan, J. R.; Gayen, A.; Traaseth, N. J., Correlating lipid bilayer fluidity with sensitivity and resolution of polytopic membrane protein spectra by solid-state NMR spectroscopy, Copyright (2014), with permission from Elsevier)

and BA in Political Science) from the University of Minnesota-Duluth in 2003 and his PhD degree from the University of Minnesota-Twin Cities in 2007 in the lab of Professor Gianluigi Veglia. Current research in the Traaseth lab is focused on understanding the role of membrane protein structure and dynamics within lipid membranes.

James Banigan is a 5th-year PhD graduate student in the Department of Chemistry at New York University. He received BS degrees in Chemistry and Biological Chemistry from the University of Chicago in 2010 and carried out research in the lab of Professor Stephen Kent.

Maureen Leninger is a 3rd-year PhD graduate student in the Department of Chemistry at New York University. She received her BA degree in Biochemistry and Molecular Biology from Boston University in 2012 and carried out research in the lab of Professor Pinghua Liu.

## Related Articles

Lipid Dynamics and Protein–Lipid Interactions in Integral Membrane Proteins: Insights from Solid-State NMR; Membrane Associated Systems: Structural Studies by MAS NMR; Membrane Proteins; Aligned Membrane Proteins: Structural Studies

## References

1. D. C. Bay and R. J. Turner, *BMC Evol. Biol.*, 2009, **9**, 140.
2. S. Schuldiner, *Biochim. Biophys. Acta*, 2009, **1794**, 748.
3. M. Rapp, E. Granseth, S. Seppala, and G.von Heijne, *Nat. Struct. Mol. Biol.*, 2006, **13**, 112.
4. M. A. Kolbusz, R.ter Horst, D. J. Slotboom, and J. S. Lolkema, *J. Mol. Biol.*, 2010, **402**, 127.
5. S. Seppala, J. S. Slusky, P. Lloris-Garcera, M. Rapp, and G.von Heijne, *Science*, 2010, **328**, 1698.
6. I. Ubarretxena-Belandia, J. M. Baldwin, S. Schuldiner, and C. G. Tate, *EMBO J.*, 2003, **22**, 6175.
7. C. G. Tate, E. R. Kunji, M. Lebendiker, and S. Schuldiner, *EMBO J.*, 2001, **20**, 77.
8. Y. J. Chen, O. Pornillos, S. Lieu, C. Ma, A. P. Chen, and G. Chang, *Proc. Natl. Acad. Sci. U. S. A.*, 2007, **104**, 18999.
9. M. K. Cho, A. Gayen, J. R. Banigan, M. Leninger, and N. J. Traaseth, *J. Am. Chem. Soc.*, 2014, **136**, 8072.
10. A. Gayen, J. R. Banigan, and N. J. Traaseth, *Angew. Chem. Int. Ed. Engl.*, 2013, **52**, 10321.
11. E. A. Morrison, G. T. DeKoster, S. Dutta, R. Vafabakhsh, M. W. Clarkson, A. Bahl, D. Kern, T. Ha, and K. A. Henzler-Wildman, *Nature*, 2012, **481**, 45.
12. S. T. Amadi, H. A. Koteiche, S. Mishra, and H. S. McHaourab, *J. Biol. Chem.*, 2010, **285**, 26710.
13. Y. S. Ong, A. Lakatos, J. Becker-Baldus, K. M. Pos, and C. Glaubitz, *J. Am. Chem. Soc.*, 2013, **135**, 15754.
14. I. Lehner, D. Basting, B. Meyer, W. Haase, T. Manolikas, C. Kaiser, M. Karas, and C. Glaubitz, *J. Biol. Chem.*, 2008, **283**, 3281.
15. T. A. Cross, M. Sharma, M. Yi, and H. X. Zhou, *Trends Biochem. Sci.*, 2011, **36**, 117.
16. A. Naito, *Solid State Nucl. Magn. Reson.*, 2009, **36**, 67.

17. A. A. De Angelis, S. C. Howell, A. A. Nevzorov, and S. J. Opella, *J. Am. Chem. Soc.*, 2006, **128**, 12256.
18. R. Verardi, L. Shi, N. J. Traaseth, N. Walsh, and G. Veglia, *Proc. Natl. Acad. Sci. U. S. A.*, 2011, **108**, 9101.
19. N. J. Traaseth, L. Shi, R. Verardi, D. G. Mullen, G. Barany, and G. Veglia, *Proc. Natl. Acad. Sci. U. S. A.*, 2009, **106**, 10165.
20. U. H. Durr, K. Yamamoto, S. C. Im, L. Waskell, and A. Ramamoorthy, *J. Am. Chem. Soc.*, 2007, **129**, 6670.
21. Y. Miao, H. Qin, R. Fu, M. Sharma, T. V. Can, I. Hung, S. Luca, P. L. Gor'kov, W. W. Brey, and T. A. Cross, *Angew. Chem. Int. Ed. Engl.*, 2012, **51**, 8383.
22. S. Abu-Baker, J. X. Lu, S. Chu, K. K. Shetty, P. L. Gor'kov, and G. A. Lorigan, *Protein Sci.*, 2007, **16**, 2345.
23. R. W. Knox, G. J. Lu, S. J. Opella, and A. A. Nevzorov, *J. Am. Chem. Soc.*, 2010, **132**, 8255.
24. D. S. Thiriot, A. A. Nevzorov, and S. J. Opella, *Protein Sci.*, 2005, **14**, 1064.
25. J. Hu, T. Asbury, S. Achuthan, C. Li, R. Bertram, J. R. Quine, R. Fu, and T. A. Cross, *Biophys. J.*, 2007, **92**, 4335.
26. J. Wang, J. Denny, C. Tian, S. Kim, Y. Mo, F. Kovacs, Z. Song, K. Nishimura, Z. Gan, R. Fu, J. R. Quine, and T. A. Cross, *J. Magn. Reson. (San Diego, Calif.: 1997)*, 2000, **144**, 162.
27. F. M. Marassi and S. J. Opella, *J. Magn. Reson.*, 2000, **144**, 150.
28. V. V. Vostrikov, C. V. Grant, S. J. Opella, and R. E.Koeppe 2nd, *Biophys. J.*, 2011, **101**, 2939.
29. B. A. Lewis, G. S. Harbison, J. Herzfeld, and R. G. Griffin, *Biochemistry*, 1985, **24**, 4671.
30. S. D. Cady, C. Goodman, C. D. Tatko, W. F. DeGrado, and M. Hong, *J. Am. Chem. Soc.*, 2007, **129**, 5719.
31. B. B. Das, H. J. Nothnagel, G. J. Lu, W. S. Son, Y. Tian, F. M. Marassi, and S. J. Opella, *J. Am. Chem. Soc.*, 2012, **134**, 2047.
32. J. R. Banigan, A. Gayen, and N. J. Traaseth, *Biochim Biophys Acta*, 2015, **1848**, 334.
33. A. A. Nevzorov, *J. Magn. Reson.*, 2014, **249**, 9.
34. A. E. McDermott, *Curr. Opin. Struct. Biol.*, 2004, **14**, 554.
35. M. Hong, Y. Zhang, and F. Hu, *Annu. Rev. Phys. Chem.*, 2011, **63**, 1.
36. M. Renault, A. Cukkemane, and M. Baldus, *Angewandte Chemie(International ed.in English)*, 2010, **49**, 8346.
37. M. Tang, D. A. Berthold, and C. M. Rienstra, *J. Phys. Chem. Lett.*, 2011, **2**, 1836.
38. D. B. Good, S. Wang, M. E. Ward, J. Struppe, L. S. Brown, J. R. Lewandowski, and V. Ladizhansky, *J. Am. Chem. Soc.*, 2014, **136**, 2833.
39. L. Shi, I. Kawamura, K. H. Jung, L. S. Brown, and V. Ladizhansky, *Angew. Chem. Int. Ed. Engl.*, 2011, **50**, 1302.
40. I. J. Lowe, *Phys. Rev. Lett.*, 1959, **2**, 285.
41. E. R. Andrew, A. Bradbury, and R. G. Eades, *Nature*, 1958, **182**, 1659.
42. T. V. Can, M. Sharma, I. Hung, P. L. Gor'kov, W. W. Brey, and T. A. Cross, *J. Am. Chem. Soc.*, 2012, **134**, 9022.
43. N. J. Traaseth, J. J. Buffy, J. Zamoon, and G. Veglia, *Biochemistry*, 2006, **45**, 13827.
44. S. H. Park, A. A. Mrse, A. A. Nevzorov, A. A. De Angelis, and S. J. Opella, *J. Magn. Reson.(San Diego, Calif.: 1997)*, 2006, **178**, 162.
45. A. A. Nevzorov, A. A. DeAngelis, S. H. Park, and S. J. Opella, Uniaxial Motional Averaging of the Chemical Shift Anisotropy of Membrane Proteins in Bilayer Environments, in NMR Spectroscopy of Biological Solids, ed. A. Ramamoorthy, CRC Press: Boca Raton, 2005, Chapter 7, pp. 177–190.
46. P. C.van der Wel, N. D. Reed, D. V. Greathouse, and R. E.Koeppe 2nd, *Biochemistry*, 2007, **46**, 7514.
47. S. Chu, A. T. Coey, and G. A. Lorigan, *Biochim. Biophys. Acta*, 2010, **1798**, 210.
48. M. P. Bhate, B. J. Wylie, L. Tian, and A. E. McDermott, *J. Mol. Biol.*, 2010, **401**, 155.
49. T. Gopinath and G. Veglia, *J. Am. Chem. Soc.*, 2009, **131**, 5754.
50. H. Yerushalmi and S. Schuldiner, *J. Biol. Chem.*, 2000, **275**, 5264.
51. S. J. Fleishman, S. E. Harrington, A. Enosh, D. Halperin, C. G. Tate, and N. Ben-Tal, *J. Mol. Biol.*, 2006, **364**, 54.
52. J. Becker-Baldus and C. Glaubitz, *Springer Ser. Biophys.*, 2014, **17**, 249.
53. C. Glaubitz, A. Groger, K. Gottschalk, P. Spooner, A. Watts, S. Schuldiner, and H. Kessler, *FEBS Lett.*, 2000, **480**, 127.
54. M. V. Korkhov and C. G. Tate, *J. Mol. Biol.*, 2008, **377**, 1094.
55. C. G. Tate, I. Ubarretxena-Belandia, and J. M. Baldwin, *J. Mol. Biol.*, 2003, **332**, 229.
56. B. E. Poulsen, F. Cunningham, K. K. Lee, and C. M. Deber, *J. Bacteriol.*, 2011, **193**, 5929.
57. B. E. Poulsen, A. Rath, and C. M. Deber, *J. Biol. Chem.*, 2009, **284**, 9870.
58. J. R. Banigan, A. Gayen, M. K. Cho, and N. J. Traaseth, *J. Biol. Chem.*, 2015, **290**, 805.
59. O. Jardetzky, *Nature*, 1966, **211**, 969.
60. E. R.de Azevedo, T. J. Bonagamba, and K. Schmidt-Rohr, *J. Magn. Reson.*, 2000, **142**, 86.
61. W. P. Jencks, *Methods Enzymol.*, 1989, **171**, 145.
62. R. M. Krupka, *Biochim. Biophys. Acta*, 1993, **1183**, 105.
63. S. S. Mordoch, D. Granot, M. Lebendiker, and S. Schuldiner, *J. Biol. Chem.*, 1999, **274**, 19480.
64. S. Dutta, E. A. Morrison, and K. A. Henzler-Wildman, *Biophys. J.*, 2014, **107**, 613.
65. E. A. Morrison and K. A. Henzler-Wildman, *J. Biol. Chem.*, 2014, **289**, 6825.
66. V. Agarwal, U. Fink, S. Schuldiner, and B. Reif, *Biochim. Biophys. Acta*, 2007, **1768**, 3036.
67. M. Baldus, A. T. Petkova, J. H. Herzfeld, and R. G. Griffin, *Mol. Phys.*, 1998, **95**, 1197.
68. J. Schaefer, R. A. McKay, and E. O. Stejskal, *J. Magn. Reson.*, 1979, **34**, 443.
69. J. R. Banigan and N. J. Traaseth, *J. Phys. Chem. B*, 2012, **116**, 7138.
70. E. Kupce, L. E. Kay, and R. Freeman, *J. Am. Chem. Soc.*, 2010, **132**, 18008.
71. J. R. Banigan, A. Gayen, and N. J. Traaseth, *J. Biomol. NMR*, 2013, **55**, 391.
72. N. J. Traaseth and G. Veglia, *J. Magn. Reson.*, 2011, **211**, 18.